EFFICIENT REPRESENTATION OF HEAD-RELATED TRANSFER FUNCTIONS IN SUBBANDS

Damián Marelli[1,2], *Robert Baumgartner*[2] *and Piotr Majdak*[2]

[1]School of Electrical Engineering and Computer Science, University of Newcastle, Australia.
[2]Acoustics Research Institute, Austrian Academy of Sciences.

ABSTRACT

Head-related transfer functions (HRTFs) describe the acoustic filtering of incoming sounds by the human morphology. We propose three algorithms for representing HRTFs in subbands, i.e., as an analysis filterbank (FB) followed by a transfer matrix and a synthesis FB. These algorithms can be combined to achieve different design objectives. In the first algorithm, the choice of FBs is fixed, and a sparse approximation procedure minimizes the complexity of the transfer matrix associated to each HRTF. The other two algorithms jointly optimize the FBs and transfer matrices. The first variant aims at minimizing the complexity of the transfer matrices, while the second one does it for the FBs. Numerical experiments show that the proposed methods offer significant computational savings when compared with other available approaches.

Index Terms— Head-related transfer functions, subband signal processing, sparse approximation.

1. INTRODUCTION

Head-related transfer functions (HRTFs) describe the acoustic filtering of incoming sounds by the torso, head, and pinna in terms of a linear-time-invariant system [1]. With a listener-specific HRTF set, the listener is immersed into a virtual auditory environment [2]. Rendering complex environments in real time with multiple virtual sources and room reflections is computationally demanding and raises the desire of an efficient representation of HRTFs.

Efficient HRTF filtering can be achieved using pole-zero (PZ) modeling [3], but this approach is inappropriate for commutation of filters when processing moving sound sources [4]. This limitation is avoided by using zero- or low-delay fast convolution (ZDFC, LDFC) [5], which permits accommodating a trade-off between efficiency and latency. It was recently shown that a better trade-off can be achieved using the subband (SB) representation [6, 7]. In that approach, an HRTF is represented as an analysis filterbank (FB) followed by a transfer matrix called subband model (SBM) and a synthesis FB. Since the analysis and synthesis FBs are common to all HRTFs within a set, the synthesis FB needs to be computed only once per audio output channel, i.e., ear signal, and its complexity is minor. Further, each analysis FB needs to be evaluated only once per audio input channel, i.e., virtual source signal, regardless of the number of reflections.

In this study we propose three algorithms for efficient representation of HRTFs in subbands. They aim at maximizing computational efficiency while focusing on perceptually relevant features. In particular, perceptual relevance is considered in terms of non-linear frequency and amplitude scaling [8] as well as phase sensitivity in humans [9]. The first algorithm relies on fixed FBs and minimizes the complexity (i.e., the number of non-zero entries) of the SBMs. The second method minimizes the support of all the SBMs in an HRTF set. It does so while including the FBs within the optimization procedure. This increases the optimization flexibility. The third method jointly optimizes the FBs and component SBMs in order to reduce the FB complexity. These three algorithms can be combined depending on design goals.

The proposed algorithms have a common initialization stage. This is based on the algorithm from [6, S5], which was designed to minimize a linear amplitude error criterion, and minimization of a logarithm criterion was achieved by repeated applications of it. As opposite, the algorithm proposed here is directly designed to minimize a logarithm criterion, and produces SBMs of significantly lower complexity.

Notation: Given a time sequence $x(t)$, $t \in \mathbb{Z}$, we use $x(\omega)$, $\omega \in (-\pi, \pi]$ to denote its discrete-time Fourier transform. Also, when it is clear from the context, we use x to denote either $x(t)$ or $x(\omega)$. The i-th entry of vector $\mathbf{a}$ is denoted by $[\mathbf{a}]_i$ and the (i, j)-th entry of matrix $\mathbf{A}$ by $[\mathbf{A}]_{i,j}$.

2. SYSTEM APPROXIMATION USING SUBBANDS

The input/output relation of a linear system with frequency response $g(\omega)$ is given by

$$y(\omega) = g(\omega)x(\omega). \quad (1)$$

This study was supported by the Austrian Science Fund (FWF, projects P24124 and M1230).

The same system can be approximately implemented in the subband domain as follows [6]:

$$\begin{aligned} \boldsymbol{\xi}(\omega) &= \downarrow_D \{\mathbf{h}(\omega)x(\omega)\} && (2)\\ \hat{\boldsymbol{\psi}}(\omega) &= \mathbf{S}(\omega)\boldsymbol{\xi}(\omega), && (3)\\ \hat{y}(\omega) &= \mathbf{f}^*(\omega)\uparrow_D \left\{\hat{\boldsymbol{\psi}}(\omega)\right\}, && (4) \end{aligned}$$

where $\mathbf{h}(\omega) = [h_0(\omega), \cdots, h_{M-1}(\omega)]^T$ and $\mathbf{f}(\omega) = [f_0(\omega), \cdots, f_{M-1}(\omega)]^T$ denote the analysis and synthesis filters, respectively, M denotes the number of subbands, $\downarrow_D \{\cdot\}$ denotes the downsampling operation with factor $D \leq M$ (i.e., keeping one out of D samples), $\uparrow_D \{\cdot\}$ denotes the upsampling operation of factor D (i.e., inserting $D-1$ zero-valued samples between every two samples), $\mathbf{S}(\omega)$ denotes the SBM, $\boldsymbol{\xi}(\omega)$ and $\hat{\boldsymbol{\psi}}(\omega)$ denote the subband representation of the input $x(\omega)$ and the approximated output $\hat{y}(\omega)$, respectively, and * denotes transpose conjugation. We choose $h_m(\omega) = h\left(\omega - 2\pi\frac{m-1}{M}\right)$ and $f_m(\omega) = f\left(\omega - 2\pi\frac{m-1}{M}\right)$, for some prototype finite impulse response filters h and f, of tap size l_h and l_f, respectively. We call (2) the analysis stage and (4) the synthesis stage.

From [6, S 3.1], it follows that

$$\hat{y}(t) = \sum_{\tau\in\mathbb{Z}} \hat{g}_{t \bmod D}(\tau)x(t-\tau),$$

where the impulse responses $\hat{g}_d$, $d = 0, \cdots, D-1$, are

$$\hat{g}_d(tD + e - d) = \left[\hat{\mathbf{G}}(t)\right]_{d,e}, \qquad (5)$$

for all $d, e = 0, \cdots, D-1$ and

$$\hat{\mathbf{G}}(\omega) = \mathbf{F}^*(\omega)\mathbf{S}(\omega)\mathbf{H}(\omega), \qquad (6)$$

with $\mathbf{H}(\omega)$ and $\mathbf{F}(\omega)$ being the polyphase representations [10] of the analysis and synthesis FBs, respectively. Hence, the scheme (2)-(4) behaves as the circular switch of D linear systems. It also has an unavoidable latency. If the prototypes h and f are chosen to be anti-causal, as we do in this work, this latency is given by

$$\Delta = D\delta_S + l_h, \qquad (7)$$

δ_S is the maximum non-causality over all the entries of $\mathbf{S}(t)$.

Using [11], and assuming that M is a power of two, so that an M-point FFT requires $M\log_2 M$ (real) multiplications [5], the implementation of the analysis FB requires

$$\Psi_{\text{FB}}(h) = \frac{l_h + M\log_2 M}{D},$$

real multiplications per (fullband) sample. The same applies to the synthesis FB, with l_f replacing l_h. Also, assuming that the input signal $x(t)$ is real valued, only half of the SBM $\mathbf{S}(t)$ entries need to be computed. Then,

$$\Psi_{\text{SBM}}(\mathbf{S}) = \frac{\#\{\mathbf{S}\}}{D}, \qquad (8)$$

where $\#\{\mathbf{S}\} = \|\Re\{\mathbf{S}\}\|_0 + \|\Im\{\mathbf{S}\}\|_0$ denotes the number of non-zero entries of $\mathbf{S}(t)$, considering the real and imaginary parts of complex entries as two different coefficients.

3. PROBLEM DESCRIPTION

Let $g^{(l)}(\omega)$, $l = 1, \cdots, L$, be a set of HRTFs. For each, l, we want to approximate $g^{(l)}$ using (2)-(4). Suppose that M, D, h and f are given, and that for each $l = 1, \cdots, L$, we have a SBM $\mathbf{S}^{(l)}$. Let $\mathbf{S} = \left\{\mathbf{S}^{(1)}, \cdots, \mathbf{S}^{(L)}\right\}$ and $\Xi = \{\mathbf{S}, h, f\}$. The error $\Upsilon^{(l)}(\Xi)$ in approximating $g^{(l)}$ is given by

$$\Upsilon^{(l)}(\Xi) = \kappa \sum_{d=0}^{D-1} \int_{-\pi}^{\pi} w(\omega) \left|\log g^{(l)}(\omega) - \log \hat{g}_d^{(l)}(\omega)\right|^2 d\omega,$$

with $\hat{g}_d^{(l)}(\omega)$ being defined as in (5)-(6) but using $\mathbf{S}^{(l)}$ in place of $\mathbf{S}$. Also, $\kappa = 200/\left(\pi D \log^2 10\right)$, and $w(\omega)$ is a frequency weighting function used to measure the approximation error in a non-linear frequency scale, e.g., Bark, equivalent rectangular bandwidth (ERB), etc. We would then like to solve

$$\begin{array}{rrcl} & \Xi_{\text{opt}} & = & \arg\min\limits_{\Xi} \Psi(\Xi) \\ \text{subject to} & \Upsilon^{(l)}(\Xi) & \leq & \epsilon, \forall l \in \{1, \cdots, L\}, \\ & \Delta^{(l)}(\Xi) & \leq & \tau, \forall l \in \{1, \cdots, L\}, \end{array} \qquad (9)$$

where $\Delta^{(l)}(\Xi)$ denotes the latency (7) of the subband implementation of $g^{(l)}$, and

$$\Psi(\Xi) = \sum_{l=1}^{L} \Psi_{\text{SBM}}\left(\mathbf{S}^{(l)}\right) + a\Psi_{\text{FB}}(h) + b\Psi_{\text{FB}}(f), \qquad (10)$$

is a measure of the complexity of the whole scheme, with $a, b \geq 0$ being constants chosen to weight the complexities of the analysis and synthesis FB, respectively.

The functions $\Psi(\Xi)$ and $\Upsilon^{(l)}(\Xi)$, $l = 1, \cdots, L$, are neither convex, nor quasi-convex. Hence, (9) cannot be solved using standard optimization algorithms, and convergence to the global optimal solution cannot be guaranteed. We propose below approximate algorithms for solving (9).

4. DESIGN WITH FIXED FILTERBANKS

Let M and D be given. In view of (8), for each $l = 1, \cdots, L$, we need to minimize the number $\#\left\{\mathbf{S}^{(l)}\right\}$ of non-zero entries of $\mathbf{S}^{(l)}$. To this end, we choose the FB prototypes h and f so that the entries of each $\mathbf{S}^{(l)}$ are concentrated on the main diagonal. Following [6, S 4.5], we design h using a root raised cosine window with inflection angular frequency $\omega_0 = \pi/M$ and roll-off factor $\beta = M/D - 1$, whose impulse response is symmetrically truncated so that energy outside the band $[-\pi/D, \pi/D]$ is below certain prescribed threshold ϑ, and we put $f = h$. With this choice of FBs, the last two terms in (10) are fixed. Hence, the design of each SBM can be addressed separately. Thus, for each $l = 1, \cdots, L$, we need to solve

$$\begin{aligned} \hat{\mathbf{S}}^{(l)} &= \arg\min_{\mathbf{S}^{(l)}} \# \left\{ \mathbf{S}^{(l)} \right\} \\ \text{subject to} \quad \Upsilon^{(l)}(\Xi) &\leq \epsilon, \quad \Delta^{(l)}(\Xi) \leq \tau. \end{aligned} \tag{11}$$

We propose below a method for solving (11). The method is formed by two stages. The first is an initialization stage, consisting in an iterative algorithm in which the number of non-zero entries of $\mathbf{S}^{(l)}$ is increased at each iteration, until the constraint $\Upsilon^{(l)}(\Xi) \leq \epsilon$ is met. This is done while respecting the constraint $\Delta^{(l)}(\Xi) \leq \tau$ at each iteration (obviously, the iterations will never end if both constraints are such that the problem is unfeasible). This algorithm chooses the support of $\mathbf{S}^{(l)}$ in a greedy fashion, i.e., choosing at each iteration the 'best' next entry. However, there is no guarantee that the set of chosen entries is the best one. Hence, we use the obtained SBM $\mathbf{S}^{(l)}$ to initialize the algorithm of the second stage. This solves a sequence of constrained optimization problems, aiming to reduce the support obtained from the first-stage algorithm. To simplify the notation, we drop the superindex $^{(l)}$ in the remainder of this section.

4.1. Initialization algorithm

This algorithm proceeds in iterations. Let $\mathbf{S}_k$ denote the SBM at the k-th iteration, and $\hat{\mathbf{G}}_k$ and $\hat{g}_{d,k}$ be defined as in (5)-(6) by using $\mathbf{S}_k$ in place of $\mathbf{S}$. For each entry $[\mathbf{S}_k]_{m,n}(t)$ of the impulse response of $\mathbf{S}_k$, we consider its real and imaginary components separately. Hence, we define a *subband index* as a quartet (m, n, t, ρ), where $\rho \in \{\Re, \Im\}$ indicates if the index corresponds to the real or the imaginary component of $[\mathbf{S}_k]_{m,n}(t)$. For each $1 \leq m \leq M$, let $\overline{m} = \operatorname{mod}(M + 1 - m, M) + 1$. Then, for each (m, n, t, ρ), we define its conjugate index by $\overline{(m, n, t, \rho)} = (\overline{m}, \overline{n}, t, \rho)$. We say that an index i is self-conjugate if $i = \overline{i}$. To each subband index $i = (m, n, t, \rho)$, we associate a real coefficient $\theta_{k,i} = \rho\left\{[\mathbf{S}_k(t)]_{m,n}\right\}$. Since the impulse response $g(t)$ is real valued, the coefficient $\theta_{\overline{i}}$ associated the the conjugate of index i is given by

$$\theta_{k,\overline{i}} = \begin{cases} \theta_{k,i}, & \rho = \Re, \\ -\theta_{k,i}, & \rho = \Im. \end{cases} \tag{12}$$

Hence, we only consider indexes $i = (m, n, t, \rho)$ with $1 \leq m, n \leq M/2 + 1$ or $2 \leq m \leq M/2$, and such that $\rho = \Re$ whenever i is self-conjugate. We call such indexes, *essential subband indexes*. We use $\mathcal{E}$ to denote the set of essential subband indexes, $\mathcal{S} = \{i \in \mathcal{E} : i = \overline{i}\}$ to denote the set of self-conjugate indexes in $\mathcal{E}$, and $\mathcal{S}^c$ to denote its complement in $\mathcal{E}$. We also use $\mathcal{R} = \{(m, n, t, \rho) \in \mathcal{E} : \rho = \Re\}$ and $\mathcal{I} = \{(m, n, t, \rho) \in \mathcal{E} : \rho = \Im\}$ to denote the set of real and imaginary indexes in $\mathcal{E}$, respectively. Notice that, in view of (12), $\mathcal{S} \subseteq \mathcal{R}$.

Let $\mathcal{H}_k = \operatorname{supp}(\mathbf{S}_k)$ denote the *support* of $\mathbf{S}_k$, i.e., the set of essential subband indexes $(m, n, t, \rho) \in \mathcal{E}$ such that $\rho\left\{[\mathbf{S}(t)]_{m,n}\right\} \neq 0$. Notice that, in view of (7), the delay constraint in (11) requires that $\delta_s \leq \frac{\tau - l_h}{D}$.

We can now introduce the initialization algorithm:

Initialization algorithm: The inputs of the algorithm are M, D, τ, ϵ and ϑ. *Design* $h = f$ *using a* root raised cosine window with $\omega_0 = \pi/M$ and $\beta = M/D - 1$, truncated so that the energy outside the band $[-\pi/D, \pi/D]$ is below ϑ. Put $\mathbf{S}_0 = 0$. Then, for each $k \in \mathbb{N}$:

1. Pick a new subband index $(m_k, n_k, t_k, \rho_k) \in \mathcal{S}$, with $t_k \geq \frac{\tau - l_h}{D}$, and add it to the current support, i.e., $\mathcal{H}_k = \mathcal{H}_{k-1} \cup \{(m_k, n_k, t_k, \rho_k)\}$ (see below how);
2. Use a gradient search method [12] to solve
$$\mathbf{S}_k = \arg\min_{\operatorname{supp}(\mathbf{S}) = \mathcal{H}_k} \Upsilon(\mathbf{S}, h, f), \tag{13}$$
3. Stop if $\Upsilon(\mathbf{S}_k, h, f) \leq \epsilon$.

The output of the algorithm is $\mathbf{S}_k$. □

We explain below how to carry out Step 1 in the initialization algorithm. Following an argument similar to the one in [6, S5], we obtain

$$\Upsilon(\Xi) = \frac{1}{D} \left\| \tilde{\mathbf{C}}_k \right\|_{\mathbf{W}}^2, \tag{14}$$

where, for all $d, e = 1, \cdots, D$, $\left[\tilde{\mathbf{C}}_k(t)\right]_{d,e} = \tilde{c}_{d,k}(tD + e - d)$, $\tilde{c}_{d,k}(\omega) = \log g(\omega) - \log \hat{g}_{d,k}(\omega)$, $\mathbf{W}(\omega)$ is the polyphase representation of $w(\omega)$, $\|\mathbf{X}\|_{\mathbf{W}}^2 = \langle \mathbf{X}, \mathbf{X} \rangle_{\mathbf{W}}$ and $\langle \mathbf{X}, \mathbf{Y} \rangle_{\mathbf{W}} = \frac{1}{2\pi} \int_{-\pi}^{\pi} \operatorname{Tr}\{\mathbf{X}(\omega)\mathbf{W}(\omega)\mathbf{Y}^\star(\omega)\} d\omega$. Now, at iteration k, we have

$$\begin{aligned} \tilde{\mathbf{C}}_k(\omega) &= \left(\mathbf{G}(\omega) - \hat{\mathbf{G}}_k(\omega)\right) \mathbf{Z}_k(\omega), \\ \mathbf{Z}_k(\omega) &= \left(\mathbf{G}(\omega) - \hat{\mathbf{G}}_k(\omega)\right)^{-1} \tilde{\mathbf{C}}_k(\omega), \end{aligned} \tag{15}$$

where $\mathbf{G}(\omega)$ denotes the polyphase representation [10] of $g(\omega)$. By approximating $\mathbf{Z}_k$ with $\mathbf{Z}_{k-1}$, we can write (14) in a linear least-squares form as follows

$$\Upsilon_{\text{lls}}(\mathbf{S}_k) = \frac{1}{D} \|\mathbf{G} - \mathbf{F}^* \mathbf{S}_k \mathbf{H}\|_{\mathbf{R}_{k-1}}^2. \tag{16}$$

with $\mathbf{R}_k(\omega) = \mathbf{Z}_k(\omega)\mathbf{W}(\omega)\mathbf{Z}_k^*(\omega)$.

To choose the next subband index, in view of (12), we associate to each index $i = (\mu, \nu, \lambda, \rho) \in \mathcal{E}$ a SBM $\mathbf{U}_i(\omega)$, defined by

$$\mathbf{U}_i(t) = \begin{cases} \mathbf{E}_{\mu,\nu,\lambda}(t), & i \in \mathcal{S}, \\ \mathbf{E}_{\mu,\nu,\lambda}(t) + \mathbf{E}_{\bar{\mu},\bar{\nu},\lambda}(t), & i \in \mathcal{S}^c \cap \mathcal{R}, \\ j\left(\mathbf{E}_{\mu,\nu,\lambda}(t) - \mathbf{E}_{\bar{\mu},\bar{\nu},\lambda}(t)\right), & i \in \mathcal{S}^c \cap \mathcal{I}, \end{cases}$$

where the impulse response $[\mathbf{E}_{\mu,\nu,\lambda}(t)]_{m,n} = 1$ if $(\mu,\nu,\lambda) = (m,n,t)$ and 0 otherwise. Also, for each $i \in \mathcal{E}$, we define $\mathbf{V}_i(\omega) = \mathbf{F}^*(\omega)\mathbf{U}_i(\omega)\mathbf{H}(\omega)$. Then, in view of (16), we choose the index $i_k \in \mathcal{E}$ for which the correlation (weighted by $\mathbf{R}_{k-1}$) between $\mathbf{V}_i(\omega)$ and the current residual $\mathbf{G}(\omega) - \hat{\mathbf{G}}_{k-1}(\omega)$ is maximized, i.e.,

$$i_k = \arg\max_{i\in\mathcal{E}} \|\mathbf{V}_i\|^{-1}_{\mathbf{R}_{k-1}} \left| \left\langle \mathbf{G} - \hat{\mathbf{G}}_{k-1}, \mathbf{V}_i \right\rangle_{\mathbf{R}_{k-1}} \right| \tag{17}$$

4.2. Main algorithm

From the initialization algorithm we obtain a SBM $\mathbf{S}$ together with its support set $\mathcal{H} = \mathrm{supp}(\mathbf{S})$. The algorithm described in this section aims to reduce the size $\#\{\mathbf{S}\}$ of $\mathcal{H}$. We have

$$\#\{\mathbf{S}\} = \sum_{(m,n,t,\rho)\in\mathcal{H}} \chi\left(\rho\left\{[\mathbf{S}(t)]_{m,n}\right\}\right),$$

where $\chi(z) = 0$ if $z = 0$ and 1 otherwise. The difficulty in minimizing $\#\left\{\mathbf{S}^{(l)}\right\}$ arises as χ is constant almost everywhere. To go around this, following [13], we choose $\alpha > 0$, and replace χ by

$$r_\alpha(z) = 1 - e^{-\frac{z^2}{2\alpha^2}},$$

which is a smooth function for each $\alpha > 0$, and converges in a point-wise manner to χ. This gives the following algorithm:
Algorithm 1: The inputs of the algorithm are M, D, ϵ, τ, ϑ and a threshold $0 < \varsigma < 1$. Run the initialization algorithm to obtain h, f, $\mathbf{S}$ and $\mathcal{H}$. Put $\mathbf{S}_0 = \mathbf{S}$ and $\alpha_0 = \|\mathbf{S}\|_\infty \triangleq \max_{m,n,t,\rho}\left|\rho\left\{[\mathbf{S}]_{m,n}(t)\right\}\right|$. Then, for each $k \in \mathbb{N}$:

1. Use the barrier method [14, S11.3], initialized using $\mathbf{S}_{k-1}$, to solve

$$\begin{array}{rl} \mathbf{S}_k = & \arg\min_{\mathrm{supp}(\mathbf{S})=\mathcal{H}} R_\alpha(\mathbf{S}) \\ \text{subject to} & \Upsilon(\mathbf{S},h,f) \le \epsilon \end{array}, \tag{18}$$

   with $R_\alpha(\mathbf{S}) = \sum_{(m,n,t,\rho)\in\mathcal{H}} r_\alpha\left(\rho\left\{[\mathbf{S}(t)]_{m,n}\right\}\right)$.
2. Put $\alpha_k = 0.5\alpha_{k-1}$ and stop if $\alpha_k < 0.2\varsigma\|\mathbf{S}_{k-1}\|_\infty$.

Upon termination, make zero all entries $[\mathbf{S}_k]_{m,n}(t)$ for which $\left|[\mathbf{S}_k]_{m,n}(t)\right| \le \varsigma\|\mathbf{S}_k\|_\infty$. The output is $\mathbf{S}_k$. □

5. COMPLETE DESIGN

Algorithm 1 yields a set of SBMs $\mathbf{S} = \left[\mathbf{S}^{(1)},\cdots,\mathbf{S}^{(L)}\right]$, together with its supports $\mathcal{H} = \left\{\mathcal{H}^{(1)},\cdots,\mathcal{H}^{(L)}\right\}$ for given choices of M, D, h and f. In this section we propose two algorithms for optimizing the complete parameter set $\Xi = [\mathbf{S},h,f]$. Both use Algorithm 1 as initialization.

The first algorithm aims to reduce the supports $\mathcal{H}$, while keeping the supports $\mathcal{I}_h = \{0,\cdots,l_h-1\}$ and $\mathcal{I}_f = \{0,\cdots,l_f-1\}$, of $h(t)$ and $f(t)$, unchanged. This algorithm is similar to Algorithm 1, with the difference in that, instead of $\mathbf{S}^{(l)}$, it jointly tunes Ξ.
Algorithm 2: Put $\mathbf{S}_0 = \mathbf{S}$, $h_0 = h$, $f_0 = f$ and $\alpha_0 = \max_{l\in\{1,\cdots,L\}}\left\|\mathbf{S}^{(l)}\right\|_\infty$. Choose $0 < \varsigma < 1$. For each $k \in \mathbb{N}$:

1. Use the barrier method [14, S11.4], initialized with $[\mathbf{S}_{k-1},h_{k-1},f_{k-1}]$, to solve

$$\begin{array}{rl} \Xi_k = & \arg\min_{\mathrm{supp}(\Xi)=\{\mathcal{H},\mathcal{I}_h,\mathcal{I}_f\}} \sum_{l=1}^{L} R^{(l)}_{\alpha_{k-1}}\left(\mathbf{S}^{(l)}\right), \\ \text{subject to} & \Upsilon^{(l)}(\Xi) \le \epsilon, \forall l,\ \|h\|_2 \le 1,\ \|f\|_2 \le 1, \end{array}$$

   with $R^{(l)}_\alpha(\mathbf{S}) = \sum_{(m,n,t,\rho)\in\mathcal{H}^{(l)}} r_\alpha\left(\rho\left\{\left[\mathbf{S}^{(l)}(t)\right]_{m,n}\right\}\right)$.
2. Put $\alpha_k = 0.5\alpha_{k-1}$ and stop if $\alpha_k < 0.2\varsigma\min_{l\in\{1,\cdots,L\}}\left\|\mathbf{S}^{(l)}_k\right\|_\infty$.

Upon termination, for each $l = 1,\cdots,L$, make zero all entries $\left[\mathbf{S}^{(l)}_k\right]_{m,n}(t)$ for which $\left|\left[\mathbf{S}^{(l)}_k\right]_{m,n}(t)\right| \le \varsigma\left\|\mathbf{S}^{(l)}_k\right\|_\infty$. The output of the algorithm is $\Xi_k = [\mathbf{S}_k,h_k,f_k]$. □

The second algorithm aims to reduce the supports $\mathcal{I}_h$ and $\mathcal{I}_f$, while keeping $\mathcal{H}$ unmodified. The basic idea is to sequentially shrink l_h and l_f until the problem becomes unfeasible.
Algorithm 3: Put $\mathbf{S}_0 = \mathbf{S}$, $h_0 = h$, $f_0 = f$, $l_{h,0} = l_h$, $l_{f,0} = l_f$ and $\alpha_0 = \max_{l\in\{1,\cdots,L\}}\left\|\mathbf{S}^{(l)}\right\|_\infty$. For each $k \in \mathbb{N}$:

1. Put $l_{h,k} = l_{h,k-1} - 1$ and $l_{f,k} = l_{f,k-1} - 1$.
2. If $\Upsilon^{(l)}(\Xi_k) > \epsilon$, for some l, use the barrier method [14, S11.4], initialized with $\Xi = [\mathbf{S}_{k-1},h_{k-1},f_{k-1}]$ and $\zeta > \max_{l=1,\cdots,L}\Upsilon^{(l)}(\Xi_k) - \epsilon$, to solve

$$\begin{array}{rl} [\Xi_k,\zeta_k] = & \arg\min_{\Xi,\zeta} \zeta + \left(\|h\|_2 - 1\right)^2 + \left(\|f\|_2 - 1\right)^2, \\ \text{subject to} & \Upsilon^{(l)}(\Xi) \le \epsilon + \zeta, \forall l. \end{array}$$

3. If $\zeta_k > 0$, stop.

The output is $\Xi_{k-1} = [\mathbf{S}_{k-1},h_{k-1},f_{k-1}]$. □

6. NUMERICAL EXPERIMENTS

For the evaluation we approximate the far-field HRTFs of subject NH92, from the ARI database at `http://www.kfs.oeaw.ac.at/hrtf`. Each HRTF has a length of 192 samples at a sampling rate of 36 kHz, and its broadband delay is removed before processing. The design goal is to solve (9) with $\epsilon = 9$ (as suggested by preliminary results from subjective localization experiments) and $\tau = 2$ ms. As in [6], the frequency weighting $w(\omega)$ corresponds to the Bark frequency scale.

In the first experiment we consider the HRTFs for 34 directions, sparsely sampling the sphere. Each HRTF was approximated by four algorithms. For the LDFC algorithm [5], we truncated each impulse response such that $\epsilon < 9$, leading to a maximum length of 159 samples over the whole HRTF set. To achieve the desired latency, we use two segments of 64

	ZDFC	LDFC	SB-IRW	Alg. 1
Analysis/synthesis	57.30	43.44	11	11
Filtering (average)	43.78	11.85	7.252	3.321
Latency	0	1.78	1.67	1.67

Table 1. Complexity (real multiplications per sample) and latency (milliseconds) for the whole HRTF set.

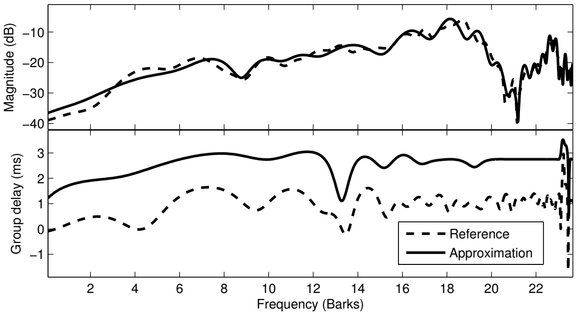

Fig. 1. An HRTF approximation example.

samples, followed by an extra segment of 128 samples. For its zero-delay (ZDFC) version we used two segments of 32 samples, the first of which is implemented using convolution, followed by another two segments of 64 and 128 samples, respectively. The remaining two methods were the iterative re-weighting subband (SB-IRW) design [6, S5] and the proposed Algorithm 1. For these methods we used $M = 32$, $D = 20$ and $l_h = l_f = 60$ (which gives $\vartheta \simeq -30$dB). The results are shown in Table 1. It shows complexity of the analysis and synthesis stages (for the LDFC and ZDFC methods, these are the FFT and IFFT operations), the filtering stage (for the SB methods, this is the average complexity of the SBMs) and the latency. We see that the SB-based methods significantly reduce the complexity of the analysis/synthesis stages, and Algorithm 1 has a clear advantage over the SB-IRW algorithm in the filtering stage. Figure 1 shows an example where the D responses of the SB implementation are averaged.

In the second experiment, to show the different performances of Algorithms 1, 2, and 3, we approximate HRTFs for virtual speakers from the 5.1-surround sound setup [15] (located at elevation 0° and azimuth 0°, ±30° and ±110°). The comparison in Table 2 shows that Algorithm 3 reduces the latency of Algorithm 1. Also, the combination of Algorithm 2 followed by Algorithm 3 reduces the filtering complexity at the expense of less latency reduction.

	Alg. 1	Alg. 3	Alg. 2+3
Analysis/synthesis	11	10	10.6
Filtering (average)	3.39	3.39	2.91
Latency	1.67	1.11	1.44

Table 2. Comparison of different subband algorithms.

REFERENCES

[1] H. Møller, M. F. Sørensen, D. Hammershøi, and C. B. Jensen, “Head-related transfer functions of human subjects,” *J Audio Eng Soc*, vol. 43, pp. 300–321, 1995.

[2] D. R. Begault, *3-D sound for virtual reality and multimedia*. Citeseer, 2000.

[3] M. Blommer and G. Wakefield, “Pole-zero approximations for head-related transfer functions using a logarithmic error criterion,” *IEEE Trans. Speech Audio Processing*, vol. 5, no. 3, pp. 278 – 87, 1997.

[4] J. Jot, V. Larcher, and O. Warusfel, “Digital signal processing issues in the context of binaural and transaural stereophony,” in *Proc. of the AES Convention*, 1995.

[5] W. Gardner, “Efficient convolution without input-output delay,” *Journal of the Audio Engineering Society*, vol. 43, no. 3, pp. 127–136, 1995.

[6] D. Marelli and M. Fu, “A recursive method for the approximation of lti systems using subband processing,” *IEEE Trans. Signal Processing*, vol. 58, no. 3, pp. 1025–1034, 2010.

[7] P. Chanda and S. Park, “Immersive Rendering of Coded Audio Streams Using Reduced Rank Models of Subband-Domain Head-Related Transfer Functions,” in *Proc. ICASSP*, 2006.

[8] B. R. Glasberg and B. C. Moore, “Derivation of auditory filter shapes from notched-noise data,” *Hearing Research*, vol. 47, pp. 103–138, 1990.

[9] B. C. Moore and B. R. Glasberg, “Difference limens for phase in normal and hearing-impaired subjects,” *J. Acoust. Soc. Am.*, vol. 86, p. 1351, 1989.

[10] P. Vaidyanathan, *Multirate Systems and Filterbanks*. Englewood Cliffs, N.J.: Prentice Hall, 1993.

[11] S. Weiss and R. Stewart, “Fast implementation of oversampled modulated filter banks,” *Electronics Letters*, vol. 36, no. 17, pp. 1502–1503, August 2000.

[12] R. Fletcher, *Practical methods of optimization*, 2nd ed., ser. A Wiley-Interscience Publication. Chichester: John Wiley & Sons Ltd., 1987.

[13] H. Mohimani, M. Babaie-Zadeh, and C. Jutten, “A fast approach for overcomplete sparse decomposition based on smoothed l^0 norm,” *IEEE Trans. Signal Processing*, vol. 57, no. 1, pp. 289–301, 2009.

[14] S. Boyd and L. Vandenberghe, *Convex Optimization*. Cambridge University Press, 2004.

[15] *Multichannel stereophonic sound system with and without accompanying picture*, Int Telecommunication Union, Geneva, Switzerland, 2012, recommendation ITU-R BS.775-3.